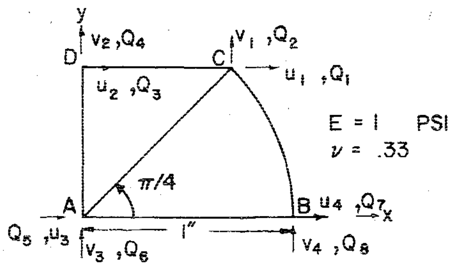

NODAL FORCE	Q_1	Q_2	Q_3	Q_4	Q_5	Q_6	Q_7	Q_8
BASED ON REF. 6	-.167	-0.800	-0.035	-0.417	0.002	0.767	0.120	0.451
INDEPENDENT $\tilde{u}_{i\sigma}$	0.120	-0.148	-0.052	-0.415	-0.164	0.410	0.095	0.153
BOUND-COLLO.	0.120	-0.148	-0.052	-0.415	-0.164	0.410	0.095	0.153

Fig. 1 Element geometry.

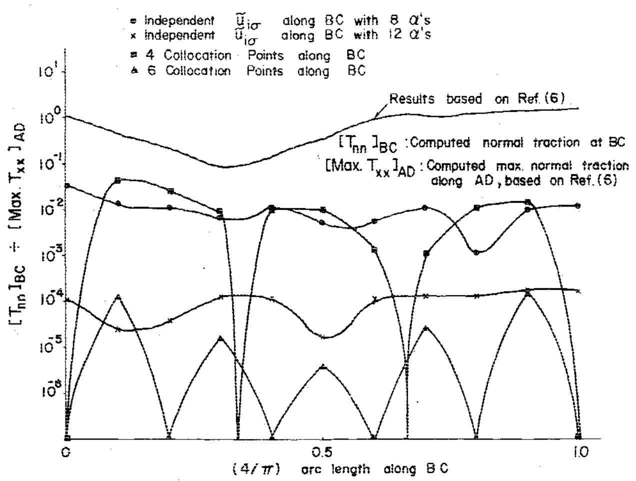

Fig. 2 Residual normal traction along BC.

arbitrary and independent of the "nodes" of the finite element at $S_{\sigma m}$. Moreover, it appears that in Ref. 8 the pointwise constraints were added to the functional in Eq. (2), thus making the formulation in Ref. 8 somewhat inconsistent.

Numerical Results

To test the efficiency of the developed procedures, a simple problem of a single plane stress finite-element $ABCD$ with eight degrees of freedom $\underset{\sim}{q}$, as shown in Fig. 1, is devised. Side BC, which is an arc of a circle, is assumed to be traction-free. The solution of the problem for prescribed displacements $u_3 = u_1 = v_1 = u_2 = v_2 = 1$ $v_3 = v_4 = u_4 = 0$ is studied. In all of the cases studied, an equilibrated element-stress field is assumed, as derived from the Airy stress function, which is a polynomial with 18 parameters $\underset{\sim}{\beta}$, consisting of complete quadratic to quintic terms in (x,y). In the formulation based on Pian and Tong,[6] using Eq. (2), the boundary displacement $\tilde{u}_{i\rho}$ all along $ABCD$ is assumed to be linear along each segment and is interpolated uniquely in terms of the nodal displacements of the respective segment. For the method involving an independently assumed $\tilde{u}_{i\sigma}$ along BC, each displacement component was assumed to be a simple polynomial in the arc length along BC, starting from a quadratic to a quintic; thus the number of α's ranged from 6 to 12. The matching points for the boudary-collection method were taken to be alternatively four and six, respectively, the points being equidistant along BC. In both of the methods, inequality (12) clearly is satisfied. Moreover, in both of the methods, $\tilde{u}_{i\rho}$ along AB, CD, and DA were assumed to be identical to that in the formulation based on Ref. 6, described previously.

The stiffness matrices obtained using the two present methods were identical to the fourth significant digit but differed significantly from that obtained through the formulation of Pian and Tong.[6] This is reflected in the general nodal forces, as shown in Fig. 1. The computed normal tractions along BC, normalized with respect to the maximum normal traction along line AD as computed through the formualtion of Ref. 6, are shown in Fig. 2. The residual tractions along BC using the formulation of Ref. 6 are seen to be of the same order as the maximum traction along AD; whereas, under both of the present formulations, they are at least an order of magnitude smaller when eight α's or four matching points are used, and, as can be seen from Fig. 2, these residual tractions are several orders of magntiude smaller when the number of α's or the number of collocation points is increased. Results similar to those in Fig. 2 were obtained for tangential tractions also but are not shown here for lack of space. Using the point-matching method for traction boundary conditions in conjunction with the hybrid-stress model, excellent results for problems of bending of plates with stress-free boundary conditions are reported in Ref. 5.

Conclusion

Two simple, efficient methods are presented to enforce, as accurately as desired, the traction boundary conditions along arbitrarily curved boundaries using the hybrid-stress finite-element model.

Acknowledgment

These results were obtained during the course of an investigation supported by the National Science Foundation under Grant NSF-ENG-74-21346.

References

[1] Atluri, S. N., *Advances in Computer Methods for Partial Differential Equations*, edited by Vichnevetsky, Rutgers University Press, New Brunswick, N. J., pp. 346-356.

[2] Pian, T. H. H., "Derivation of Element Stiffness Matrics by Assumed Stress Distributions," *AIAA Journal*, Vol. 2, July 1964, pp. 1333-1336.

[3] Tong, P. and Pian, T. H. H., *International Journal of Solids and Structures*, Vol. 5, 1969, pp. 463-472.

[4] Pian, T. H. H., Tong, P., and Luk, C. H., *Proceedings of Third Conference on Matrix Methods in Structural Mechanics*, Wright-Patterson Air Force Base, 1972.

[5] Rhee, H. C., "On the Accuracy of Finite Element Solutions of Problems of Bending of Plates with Traction Boundary Conditions," Ph.D. Thesis, Georgia, Inst. of Technology, 1977.

[6] Pian, T. H. H. and Tong, P., *International Journal of Numerical Methods in Engineering*, Vol. 1, Jan. 1969, pp. 3-28,

[7] Finlayson, B. A., *The Method of Weighted Residuals and Variational Principles*, Academic Press, New York, 1972.

[8] Wolf, J. P., "Generalized Stress Models for Finite Element Analysis," Ph.D. Thesis, ETH, Zurich, Switzerland, 1974.

Rod and Beam Finite Element Matrices and Their Accuracy

Atis A. Liepins*
Littleton Research and Engineering Corp., Littleton, Mass.

EXACT dynamic stiffness matrices for rods and beams have been given by Henshell and Warburton,[1] Akesson,[2] and others. Reference 2 includes an extensive bibliography and gives an historical perspective to this method of structural

Received April 8, 1977; revision received Jan. 6, 1978.

Index category: Structural Dynamics.

*Presently, Senior Staff Engineer, Simpson Gumpertz & Heger, Inc., Consulting Engineers, Cambridge, Mass. Member AIAA.

dynamic analysis. The purpose of this Note is to show the relationship between the exact dynamic stiffness matrix and the stiffness and mass matrices of the displacement finite element method.[3] In addition, errors in the element matrices and in the natural frequencies of some simple structures are given.

Rod Element

For a rod undergoing undamped harmonic axial motion with circular frequency ω, the end forces F_1, F_2 are related to the end displacements u_1, u_2 by a dynamic stiffness matrix[1,4] as follows:

$$\begin{Bmatrix} F_1 \\ F_2 \end{Bmatrix} = \frac{EAk}{\sin kL} \begin{bmatrix} \cos kL & -1 \\ -1 & \cos kL \end{bmatrix} \begin{Bmatrix} u_1 \\ u_2 \end{Bmatrix} \tag{1}$$

where L is the length of the rod with cross-section area A, $k=\omega/c$ is the wave number, $c^2=E/\rho$, E is Young's modulus, and ρ is mass density. End loads and displacements are positive when they point to the right in a horizontally oriented rod. Equation (1) is exact in the sense that mass discretization is not necessary to obtain accurate response. Furthermore, formulations of models using Eq. (1) have an infinite number of natural frequencies and mode shapes.

If we expand the elements of the dynamic stiffness matrix, Eq. (1), in power series of kL, we obtain:

$$\begin{Bmatrix} F_1 \\ F_2 \end{Bmatrix} = \left[\frac{EA}{L} \begin{bmatrix} 1 & -1 \\ -1 & 1 \end{bmatrix} - \frac{\rho AL\omega^2}{6} \begin{bmatrix} 2 & 1 \\ 1 & 2 \end{bmatrix} - \frac{\rho AL\omega^2 (kL)^2}{360} \begin{bmatrix} 8 & 7 \\ 7 & 8 \end{bmatrix} - \frac{\rho AL\omega^2 (kL)^4}{15120} \begin{bmatrix} 32 & 31 \\ 31 & 32 \end{bmatrix} - O(kL)^6 \right] \begin{Bmatrix} u_1 \\ u_2 \end{Bmatrix} \tag{2}$$

The first matrix on the right-hand side of Eq. (2) will be recognized as the static stiffness and the second as the consistent mass matrix.[3,5] Note that the stiffness and consistent mass matrices are obtained without the use of shape functions.[3] They are the leading terms in the expansion of the exact dynamic stiffness matrix. The third and subsequent matrices constitute the error in the dynamic stiffness of the rod in a consistent mass finite element formulation. Since the static stiffness matrix for the rod is exact, the error is in the approximation of mass and is of order $(kL)^2 = (2\pi L/\lambda)^2 = (\pi/N)^2$, where λ is the wavelength and N the number of equal length elements per half wavelength.

The error matrices of Eq. (2) may be used to estimate the error in natural frequencies of certain rod element models. Consider the special case of an end-supported rod of length L_0 approximated by N equal-length elements. For a consistent mass formulation, obtain the system kinetic energy $\omega^2 T_c$ using the second matrix, and the approximate error in kinetic energy $\omega^2 T_1$ using only the third matrix in Eq. (2). Use the exact vibration mode with amplitude u_0 to obtain displacements at the ith and neighboring grid points

$$u_i = u_0 \sin \pi x_i / L_0$$

$$u_{i+1} = u_0 \sin \pi (x_i + L)/L_0$$

Then, we have

$$\omega^2 T_c = \frac{1}{6} \rho AL\omega^2 \sum_{i=1}^{N} (u_i^2 + u_i u_{i+1} + u_{i+1}^2)$$

$$= \frac{1}{6} \rho AL\omega^2 u_0^2 S_0 [2 + \cos(\pi/N)]$$

$$\omega^2 T_1 = \frac{1}{360} \rho AL\omega^2 (kL)^2 \sum_{i=1}^{N} (4u_i^2 + 7u_i u_{i+1} + 4u_i^2)$$

$$= \frac{1}{360} \rho AL\omega^2 (\pi/N)^2 u_0^2 S_0 [8 + 7\cos(\pi/N)]$$

where

$$S_0 = \sum_{i=1}^{N} \sin^2 \pi x_i / L_0 = \sum_{i=1}^{N} \cos^2 \pi x_i / L_0 = N/2$$

$$\sum_{i=1}^{N} \sin \pi x_i / L_0 \cos \pi x_i / L_0 = 0$$

Rayleigh's principle leads to

$$\omega^2/\omega_0^2 = T_0/T_c \approx 1 + T_1/T_c$$

$$= 1 + \frac{(\pi/N)^2 [8 + 7\cos(\pi/N)]}{60[2 + \cos(\pi/N)]} \approx 1 + (\pi/N)^2/12$$

where ω_0 and $\omega_0^2 T_0$ are the exact natural frequency and kinetic energy, respectively, and T_1/T_c is the error in frequency squared. If, in addition to distributed mass, the model has equal concentrated masses at all grid points, T_1 is unchanged, T_c increases with the size of the concentrated masses, and T_1/T_c again can be used to calculate the error in frequency.

If we use lumped mass matrices, the kinetic energy is

$$\omega^2 T_L = \frac{1}{2} \rho AL\omega^2 \sum_{i=1}^{N} (u_i^2 + u_{i+1}^2) = \frac{1}{2} \rho AL\omega^2 u_0^2 S_0$$

there is an additional contribution to error due to the difference between consistent and lumped mass matrices

$$\omega^2 T_{Lc} = -\frac{1}{12} \rho AL\omega^2 \sum_{i=1}^{N} (u_i - u_{i+1})^2$$

$$= -\frac{1}{6} \rho AL\omega^2 u_0^2 S_0 [1 - \cos(\pi/N)]$$

and

$$\omega^2/\omega_0^2 \approx 1 + (T_1 + T_{Lc})/T_L \approx 1 - (\pi/N)^2/12$$

If, as is implemented in NASTRAN,[6] the mass matrix is the average of the consistent and lumped mass matrices, the kinetic energy is

$$\omega^2 T_a = \frac{1}{24} \rho AL\omega^2 \sum_{i=1}^{N} (5u_i^2 + 2u_i u_{i+1} + 5u_{i+1}^2)$$

$$= \frac{1}{12} \rho AL\omega^2 u_0^2 S_0 [5 + \cos(\pi/N)]$$

the contribution to error from the difference between the consistent and averaged mass matrices is $\omega^2 T_{ac} = \omega^2 T_{Lc}/2$, the contribution to error from the fourth matrix in Eq. (2) must also be considered,

$$\omega^2 T_2 = \frac{\rho AL\omega^2 (kL)^4}{15120} \sum_{i=1}^{N} (16u_i^2 + 31u_i u_{i+1} + 16u_{i+1}^2)$$

$$= \frac{1}{240} \rho AL\omega^2 (\pi/N)^4 u_0^2 S_0$$

and

$$\omega^2/\omega_0^2 = 1 + (T_1 + T_2 + T_{ac})/T_a \approx 1 - (\pi/N)^4/240$$

In summary, we have the following estimates for frequency error, $\epsilon = \omega/\omega_0 - 1$

Lumped mass:

$$\epsilon_L = -(\pi/N)^2/24 \tag{3}$$

Consistent mass:

$$\epsilon_c = (\pi/N)^2/24 \tag{4}$$

Averaged mass:

$$\epsilon_a = -(\pi/N)^4/480 \tag{5}$$

Error estimates (3) and (4) are in agreement with those given in Refs. 6 and 7. The magnitude of Eq. (5) agrees with that of Ref. 6 but the sign differs.

Alternatively, these error estimates can be derived from the equivalence of maximum potential and kinetic energies, from grid point equilibrium equations as was done in Ref. 7, or from finite difference equations as was done in Ref. 8.

The preceding error estimates are confirmed by calculations with NASTRAN of the natural frequencies of an end-supported uniform rod with $L_0 = 30$, $N = 30$, $E = 3600$, $\rho = A = 1$. For this rod, the analytically obtained natural frequencies are $f_n = n$, $n = 1, 2, 3 \ldots$. The error estimates, Eqs. (3-5) and those from NASTRAN calculations are compared in Table 1.

Beam Element

For a beam undergoing undamped harmonic transverse motion, the end shears V_1, V_2 and moments M_1, M_2 are related to the end displacements W_1, W_2 and rotations θ_1, θ_2 by a dynamic stiffness matrix[1,4] as follows:

$$\begin{Bmatrix} V_1/k \\ V_2/k \\ M_1 \\ -M_2 \end{Bmatrix} = \frac{EIk^2}{1 - C\chi} \times \begin{bmatrix} S\chi + C\sigma & -S-\sigma & S\sigma & C-\chi \\ -S-\sigma & S\chi + C\sigma & C-\chi & S\sigma \\ S\sigma & C-\chi & S\chi - C\sigma & S-\sigma \\ C-\chi & S\sigma & S-\sigma & S\chi - C\sigma \end{bmatrix} \begin{Bmatrix} W_1 \\ W_2 \\ \theta_1/k \\ -\theta_2/k \end{Bmatrix} \tag{6}$$

where $S = \sin kL$, $C = \cos kL$, $\sigma = \sinh kL$, $\chi = \cosh kL$, L is the length of the beam with moment of inertia I, and $k^4 = \rho A \omega^2 / EI$ is the wave number. End shears and displacements are positive when up, moments and rotations when counter clockwise.

If, as was done for the rod element, we expand the elements of Eq. (6) in power series of kL, we obtain:

$$\begin{Bmatrix} V_1 \\ V_2 \\ M_1/L \\ -M_2/L \end{Bmatrix} = \left[\frac{EI}{L^3} \begin{bmatrix} 12 & -12 & 6 & -6 \\ -12 & 12 & -6 & 6 \\ 6 & -6 & 4 & -2 \\ -6 & 6 & 2 & 4 \end{bmatrix} - \frac{\rho A L \omega^2}{420} \times \begin{bmatrix} 156 & 54 & 22 & 13 \\ 54 & 156 & 13 & 22 \\ 22 & 13 & 4 & 3 \\ 13 & 22 & 3 & 4 \end{bmatrix} - \rho A L \omega^2 (kL)^4 \frac{4/7}{11!} \times \begin{bmatrix} 25488 & 23022 & 5352 & 5043 \\ 23022 & 25488 & 5043 & 5352 \\ 5352 & 5043 & 1136 & 1097 \\ 5043 & 5352 & 1097 & 1136 \end{bmatrix} - O(kL)^8 \right] \begin{Bmatrix} W_1 \\ W_2 \\ \theta_1 L \\ -\theta_2 L \end{Bmatrix} \tag{7}$$

Again, the static stiffness and consistent mass matrices[5] result without the use of shape functions. The error in the dynamic stiffness of consistent mass beam elements is of the order $(kL)^4 = (\pi/N)^4$ and is entirely due to approximation of mass.

The second and third matrices of Eq. (7), together with the exact mode shape

$$W_i = W_0 \sin \pi x_i / L_0$$

can be used to estimate the error in the natural frequencies of simply supported beams. Proceeding as for the rod, we obtain

Lumped mass:

$$\epsilon_L = -(\pi/N)^4/1440 \tag{8}$$

Consistent mass:

$$\epsilon_c = +(\pi/N)^4/1440 \tag{9}$$

which agree with Refs. 6 and 7.

Error estimates, Eqs. (8) and (9), are confirmed by calculations with NASTRAN of the natural frequencies of a simply supported beam with $L_0 = 8$, $N = 8$, $E = 1000$, $I = 1.66046$, $\rho = A = 1$. For this beam, the analytically obtained frequencies are $f_n = n^2$ $n = 1, 2, 3 \ldots$. The error

Table 1 Errors in natural frequencies of rod models

Mode	N	Lumped mass f_n[a]	ϵ[b]	ϵ_ℓ, Eq. (3)	Consistent mass f_n[a]	ϵ[b]	ϵ_ℓ, Eq. (4)	Averaged mass f_n[a]	ϵ[b]	ϵ_ℓ, Eq. (5)
1	30	0.9995432	−0.0004569	−0.0004569	1.000461	0.000461	0.000457	0.9999998	−0.0000002	−0.0000002
2	15	1.996347	−0.001826	−0.001828	2.003657	0.001828	0.001828	1.999992	−0.000004	−0.000004
3	10	2.987678	−0.004107	−0.004112	3.012351	0.004117	0.004112	2.999939	−0.000020	−0.000020
4	7.5	3.970821	−0.007295	−0.007311	4.029304	0.007326	0.007311	3.999742	−0.000064	−0.000064
5	6	4.943080	−0.011384	−0.011423	5.057294	0.011459	0.011423	4.999209	−0.000158	−0.000157
6	5	5.901790	−0.016368	−0.016449	6.099120	0.016520	0.016449	5.998022	−0.000330	−0.000325
10	3	9.549297	−0.045070	−0.045693	10.46073	0.046073	0.045693	9.973915	−0.002608	−0.002505
15	2	13.50475	−0.099683	−0.102808	16.53987	0.102658	0.102808	14.79371	−0.013753	−0.012683
20	1.5	16.53987	−0.173006	−0.182770	23.39090	0.169545	0.182770	19.09859	−0.045070	−0.040086

[a] Frequency calculated with NASTRAN. [b] Error in f_n.

Table 2 Errors in natural frequencies of simply supported beam models

Mode	N	Lumped mass f_n [a]	Lumped mass ϵ [b]	Lumped mass ϵ_f, Eq. (8)	Consistent mass f_n [a]	Consistent mass ϵ [b]	Consistent mass ϵ_f, Eq. (9)
1	8	0.9999828	−0.0000172	−0.0000165	1.000016	0.000016	0.000016
2	4	3.998780	−0.000305	−0.000264	4.001039	0.000260	0.000264
3	8/3	8.983501	−0.001833	−0.001388	9.011579	0.001286	0.001388
4	2	15.88395	−0.007259	−0.004228	16.06315	0.003947	0.004228
5	8/5	24.42284	−0.023086	−0.010322	25.23177	0.009271	0.010322
6	4/3	33.72486	−0.063198	−0.021403	36.65781	0.018272	0.021403
7	8/7	41.65990	−0.14980	−0.039652	50.52612	0.031145	0.039652

[a] Frequency calculated with NASTRAN. [b] Error in f_n.

estimates, Eqs. (8) and (9) and those obtained from NASTRAN calculations, are compared in Table 2. The large differences between the error estimates generated by NASTRAN and those computed with Eq. (8), especially for the higher modes, are due to terms $O(kL)^8$ neglected in the kinetic energy error estimation. These terms become significant as $(\pi/N)^4$ approaches unity, that is, as the number of elements per half wavelength decreases.

References

[1] Henshell, R. D. and Warburton, G. B., "Transmission of Vibration in Beam Systems," *International Journal for Numerical Methods in Engineering*, Vol. 1, Jan. 1969, pp. 47-66.

[2] Akesson, B. A., "PFVIBAT-A Computer Program for Plane Vibration Analysis by an Exact Method," *International Journal of Numerical Methods in Engineering*, Vol. 10, June 1976, pp. 1221-1231.

[3] Zienkewicz, D. C., *The Finite Element Method in Engineering Science*, McGraw Hill, N.Y., 1971.

[4] Clough, R. W. and Penzien, J., *Dynamics of Structures*, Part 3, McGraw Hill, N.Y., 1975.

[5] Archer, J. S., "Consistent Matrix Formulations for Structural Analysis Using Finite-Element Techniques," *AIAA Journal*, Vol. 3, Oct. 1965, pp. 1910-1913.

[6] MacNeal, R. H., *The NASTRAN Theoretical Manual*, NASA SP-221(01), 1972.

[7] Walz, J. E., Fulton, R. E., Cyrus, N. J., and Eppink, R. T., "Accuracy of Finite Element Approximations to Structural Problems," NASA TN D-5728, March 1970.

[8] MacNeal, R. H., *Electric Circuit Analogies for Elastic Structures*, John Wiley & Sons, N.Y., 1962.

Pressure Dependence of Burning Rate of Composite Solid Propellants

R. P. Rastogi,* H. J. Singh,† Desh Deepak,‡ and A. K. Srivastava§
University of Gorakhpur, Gorakhpur, India

Nomenclature

a,b = constants of Eq. (15)
C_f = concentration of species f
C_{fe} = equilibrium concentration of species f at the end of chemical reaction zone
C_{fs} = concentration of species f near the propellant surface
C_s = specific heat of solid (average of fuel and oxidizer)
k_0 = rate constant at zero atmosphere
k_1 = rate constant of the first-order reaction
L = length of the chemical reaction zone
$\dot{m}$ = mass buring rate
n_f = number of moles of fuel
P = chamber pressure
Q_h = net heat release (positive) for gasification of the propellant
$\dot{r}$ = buring rate
R = gas constant
R_f = chemical reaction rate per unit volume
T_0 = ambient temperature
T_f = flame temperature at the end of chemical reaction zone
T_s = surface temperature of the burning propellant (average)
U = volume rate of flow
V = total volume of the reactor
ΔV^* = volume of activation, i.e., difference in the volumes of activate complex and the reactants
λ_{gs} = average thermal conductivity of flame gas at the surface
ρ_g = density of the gas
ρ_p = propellant density

Received May 9, 1977; revision received Jan. 23, 1978.

Index categories: Combustion and Combustor Designs; Solid and Hybrid Rocket Engines.

*Professor, Dept. of Chemistry. Associate Fellow AIAA.
†Lecturer, Dept. of Chemistry.
‡Presently at Hindustan Lever Ltd., Research Centre, Andheri (East), Bombay.
§Junior Research Fellow, Dept. of Chemistry.

Introduction

VARIOUS equations relating the burning rate of composite propellants and pressure have been proposed from time to time.[1] Attempts have been made by several workers[2-6] to develop theories of combustion of solid propellants. Rastogi et al.[7] have recently reviewed the various theories of combustion of propellants. Out of these the theory based on the granular diffusion flame model is most convenient for deducing expressions for the pressure dependence of burning rate. A wide range of experimental data is available and none of the proposed equations fits the entire range. Hence, it is desirable to re-examine the question of pressure dependence of burning rate.

We shall base our discussion on the concept of heat balance at the propellant surface, that is,

$$\dot{m}[C_s(T_s-T_0)-Q_h]=\lambda_{gs}\frac{(T_f-T_s)}{L} \tag{1}$$

In combustion theories L has been introduced in a rather phenomenological way and has been related to chemical reaction rate in a dubious manner. The pressure dependence of $\dot{m}$ appears to follow as a consequence of pressure dependence of density.[6] In the following theory, we have considered the reaction zone as a nonisothermal reactor and the pressure dependence of the reaction rate constant. $\dot{m}$ comes out to be pressure dependent on account of the latter. The theoretical results have been compared with the burning rate data at various pressures for different propellants having difference particle sizes of the oxidizer. The available ex-